

## POTENTIAL VORTICITY ASPECTS OF THE MJO

Matthew T. Masarik and Wayne H. Schubert \*  
 Colorado State University, Fort Collins, Colorado

## 1. INTRODUCTION

The Madden-Julian Oscillation (MJO) is a complex, multiscale phenomenon in which an envelope of convective clouds propagates eastward along the equator. Embedded within the convective envelope are interacting synoptic-scale, mesoscale, and cumulus scale motions. While much has been learned about the MJO, there are still many questions left to be answered. The goal of this work is to isolate an aspect of the MJO problem that has not been sufficiently explored—the extent to which the flow in the wake of the convective envelope can be interpreted as balanced and derivable from the potential vorticity field. To this end we will not treat the complex structure within the convective region, rather we will consider its net, large-scale effect.

The motivation for this approach is as follows. Balanced theories, such as quasi-geostrophic theory and semi-geostrophic theory, provide a foundation for understanding the dynamics of midlatitude weather systems. These theories are more tractable than the primitive equations and can be succinctly expressed as two equations—a prognostic equation for the material conservation of potential vorticity, and a diagnostic equation (or invertibility principle) relating the potential vorticity to the streamfunction. In many tropical weather systems, such as the ITCZ and tropical cyclones, the release of latent heat plays a crucial role, so that potential vorticity is not materially conserved. However, even in these cases, a useful strategy is to formulate a balanced model that predicts the potential vorticity and then inverts it to find the associated balanced wind and mass fields. This approach has yielded insights into the dynamics of ITCZ breakdown and the formation of easterly waves (e.g., Schubert et al. 1991) and into the extreme PV structures that evolve in tropical cyclones (e.g., Hausman et al. 2005). What about large-scale weather systems that occur on the equator, such as

the MJO? Are the concepts of balance and invertibility useful in understanding the essential dynamics of the MJO? Here we attempt to answer this question in the simplest context, i.e., in the context of a linearized equatorial  $\beta$ -plane model. The primitive equation model is discussed in section 2, where analytical solutions are attained and decomposed into the equatorial wave components. Section 3 presents an equatorial invertibility principle from which (knowing the PV field) the wake flow can be fairly accurately recovered. Section 4 identifies the convective forcing parameters that are crucial in determining the strength of the PV wake.

## 2. PRIMITIVE EQUATION MODEL

Consider small amplitude motions about a resting basic state in a stratified, compressible, quasi-static atmosphere on the equatorial  $\beta$ -plane. Using  $z = \ln(p_0/p)$  (where  $p_0 = 1010$  mb is a constant “surface” pressure) as the vertical coordinate, we can write the linearized governing equations as

$$\begin{aligned} \frac{\partial u}{\partial t} - \beta y v + \frac{\partial \phi}{\partial x} &= -\alpha u, & \frac{\partial v}{\partial t} + \beta y u + \frac{\partial \phi}{\partial y} &= -\alpha v, \\ \frac{\partial u}{\partial x} + \frac{\partial v}{\partial y} + \frac{\partial w}{\partial z} - w &= 0, & & (1) \\ \frac{\partial \phi}{\partial z} = RT, & \quad \frac{\partial T}{\partial t} + \Gamma w &= -\alpha T + \frac{Q}{c_p}, \end{aligned}$$

where  $u$  is the eastward component of velocity,  $v$  the northward component,  $w = Dz/Dt$  the “vertical log-pressure velocity,”  $\phi$  the perturbation geopotential,  $T$  the perturbation temperature,  $\beta = 2\Omega/a$  the equatorial value of the northward gradient of the Coriolis parameter,  $\Omega$  the Earth’s rotation rate,  $a$  the Earth’s radius,  $\alpha$  the constant coefficient for Rayleigh friction and Newtonian cooling,  $\Gamma = d\bar{T}/dz + \kappa\bar{T}$  ( $\kappa = R/c_p$ ) the basic state static stability computed from the basic state temperature profile  $\bar{T}(z)$ , and  $Q(x, y, z, t)$  the diabatic source term. For simplicity we assume that  $\Gamma$  is a constant, and choose the tropical tropospheric mean

---

\*Corresponding author address: Matthew T. Masarik, Department of Atmospheric Science, Colorado State University, Fort Collins, CO 80523-1375; e-mail: [mmasarik@atmos.colostate.edu](mailto:mmasarik@atmos.colostate.edu)

value  $\Gamma = 23.79$  K. We set  $\alpha = (4 \text{ days})^{-1}$ . We seek solutions of (1) on a domain that is infinite in  $y$ , periodic over  $-\pi a \leq x \leq \pi a$ , and confined between  $z = 0$  and  $z = z_T = \ln(1010/200) \approx 1.619$ , with the boundary conditions  $w = 0$  at  $z = 0, z_T$ .

## 2.1 Potential Vorticity Principle

We can derive a PV principle from (1) by first cross differentiating the horizontal momentum equation to arrive at a vorticity equation. Then combine the hydrostatic, continuity, and thermodynamic equations in such a way to eliminate  $T$  and  $w$ . Combining this result with the vorticity equation to eliminate the divergence, yields the PV principle

$$\frac{\partial q}{\partial t} + \beta v = -\alpha q + \frac{\beta y}{c_p \Gamma} \left( \frac{\partial}{\partial z} - 1 \right) Q, \quad (2)$$

where

$$q = \frac{\partial v}{\partial x} - \frac{\partial u}{\partial y} + \frac{\beta y}{R\Gamma} \left( \frac{\partial}{\partial z} - 1 \right) \frac{\partial \phi}{\partial z} \quad (3)$$

is the potential vorticity anomaly. We shall concentrate on interpreting the flow patterns associated with a moving heat source in terms of a PV wake. For this interpretation the  $y$ -factor in the last term of (2) plays a crucial role. It causes the source term  $Q$  to be ineffective at generating a PV anomaly at the equator but maximizes the PV response near the poleward edges of the heat source. In this manner a moving equatorial heat source can produce two ribbons of lower tropospheric PV anomaly, a positive one off the equator in the northern hemisphere and a negative one off the equator in the southern hemisphere, with oppositely signed PV anomalies in the upper troposphere.

## 2.2 Vertical Structure

The first step in solving (1) is vertical normal mode transforming, and assuming that the diabatic heating excites only the first vertical internal mode. It is then convenient to introduce a vertical structure function  $Z(z)$ , and its derivative  $Z'(z)$ . This function satisfies the second order equation

$$\left( \frac{d}{dz} - 1 \right) \frac{dZ}{dz} = - \left( \frac{\pi^2}{z_T^2} + \frac{1}{4} \right) Z, \quad (4)$$

and the boundary conditions  $Z'(0) = Z'(z_T) = 0$ . These two functions, normalized so that  $Z'(z)$  has

a maximum value of unity, are shown in Fig. 1. Also shown in Fig. 1 is the 120-day mean (November 1992 – February 1993) vertical profile of the heating rate for the western Pacific warm pool (Johnson and Ciesielski 2000). The observed mean profile of  $Q/c_p$  has a peak value of approximately  $4 \text{ K day}^{-1}$ , and its shape is closely approximated by  $Z'(z)$ , which is the justification for considering only the first vertical internal mode in the following analysis. Over the 120-day observational period there were two MJO passages (Lin and Johnson 1996b, Yanai et al. 2000). During these two periods of enhanced convection the shape of the vertical profile of  $Q/c_p$  was very similar to the shape of the time mean profile shown in Fig. 1, but the peak values were considerably larger,  $10 \text{ K day}^{-1}$  for the first MJO and  $16 \text{ K day}^{-1}$  for the second. Thus, for the vertical profile of heating at the time of peak convective activity during the passage of an MJO, our model uses the  $Z'(z)$  profile shown in Fig. 1, but scaled so the peak value is  $12 \text{ K day}^{-1}$  rather than  $4 \text{ K day}^{-1}$ .

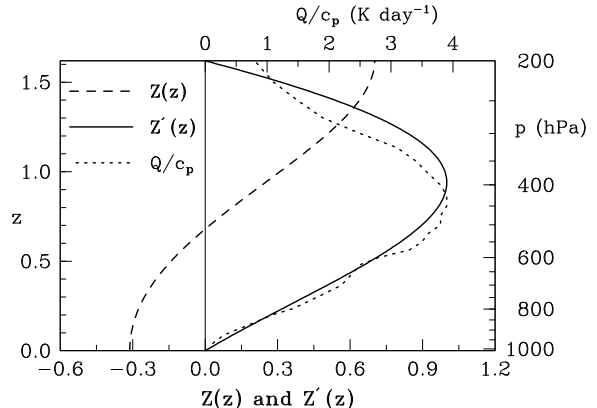


Figure 1: The curves labeled  $Z(z)$  and  $Z'(z)$  are interpreted using the lower scale. The curve labeled  $Q/c_p$  (interpreted using the upper scale) is the 120-day mean vertical profile of heating rate for the western Pacific warm pool, as determined by Johnson and Ciesielski (2000).

Assuming that  $u, v, \phi, T, w, Q$  have the separable forms

$$\begin{pmatrix} u(x, y, z, t) \\ v(x, y, z, t) \\ \phi(x, y, z, t) \end{pmatrix} = \begin{pmatrix} \hat{u}(x, y, t) \\ \hat{v}(x, y, t) \\ \hat{\phi}(x, y, t) \end{pmatrix} Z(z),$$

$$\begin{pmatrix} T(x, y, z, t) \\ w(x, y, z, t) \\ Q(x, y, z, t) \end{pmatrix} = \begin{pmatrix} \hat{T}(x, y, t) \\ \hat{w}(x, y, t) \\ \hat{Q}(x, y, t) \end{pmatrix} Z'(z),$$

we can split off the vertical dependence from (1) and are left with a system for the horizontal structure functions  $\hat{u}, \hat{v}, \hat{\phi}, \hat{T}, \hat{w}$ .

### 2.3 Forcing Function

We assume that the diabatic forcing is due to an eastward propagating region of deep convection. The exact form of the forcing is

$$\hat{Q}(x, y, t) = \frac{1}{2}Q_0 \exp \left[ - \left( \frac{y-y_0}{b_0} \right)^2 \right] \begin{cases} 1 + \cos(\pi\xi/a_0) & |\xi| \leq a_0, \\ 0 & |\xi| \geq a_0, \end{cases}$$

where  $\xi = x - ct$ ,  $c$  is the propagation speed of the cloud cluster,  $y_0$  is the displacement of its center from the equator,  $a_0$  its half-width in  $x$ ,  $b_0$  its e-folding width in  $y$ , and  $Q_0$  its peak value. It was explained previously how observations (Yanai et al. 2000) led us to our choice of  $Q_0/c_p = 12 \text{ K day}^{-1}$ . Our choice of size was guided by studies which have constructed composite MJO lifecycles from MJO filtered OLR data along the equator (e.g., Hendon and Salby 1994; Kiladis et al. 2005). Using these to estimate the zonal scale of the high intensity region within the negative OLR anomaly we get 2000–4000 km, which we hope captures the zonal extent of the convective core. We chose a somewhat arbitrary intermediate value of 2500 km ( $a_0 = 1250 \text{ km}$ ). In the composite MJO of the above mentioned studies the OLR anomaly is seen to be zonally elongated. We chose a width scale to reflect this shape (e-folding width  $b_0 = 450 \text{ km}$ ). The convective anomaly associated with the MJO moves eastward at about 5 m/s (Hendon and Salby 1994), so we set our forcing to propagate eastward at this constant speed.

### 2.4 Primitive Equation Solutions

Returning to the set of “shallow water” equations, we proceed by making a substitution for the zonal distance variable. Recall in the previous section we introduced  $\xi = x - ct$ . If we assume our solutions are in steady state translating at a constant speed  $c$ , then we can exchange the  $x$  and  $t$  dependence in our equations with just  $\xi$  dependence. This is done through the replacements  $\partial/\partial t \rightarrow -c(\partial/\partial\xi)$  and  $\partial/\partial x \rightarrow \partial/\partial\xi$ . Now our solutions will exist in a reference frame propagating eastward at a constant speed, fixed on the convective forcing. A brief summary of the mathematical solving procedure is now given (for details, see Schubert and Masarik 2006). Start by Fourier transforming in the zonal direction. Next Normal Mode transform in the meridionally direction. Performing these operations reduces our system to a set of algebraic equations in

wavenumber space for our solution vector expansion coefficient. The expansion coefficient can be determined using the prescribed form of the diabatic forcing. Using this expansion coefficient to Inverse Normal Mode transform, followed by an Inverse Fourier transform yields the horizontal structure. Reapplying the vertical structure then gives our total, steady state solutions. These solutions can be considered as the primitive equation generalization of the simplest MJO model involving the first baroclinic mode response to a moving planetary heat source under the long wave approximation (Chao 1987).

The 850 mb winds and geopotential fields are shown in the top panel of Fig. 2 for  $y_0 = 0$ . The remaining panels of Fig. 2 show the decomposition of the total fields into Rossby modes, inertia-gravity modes, and Kelvin modes. We have not plotted the contribution from mixed Rossby-gravity modes since it vanishes when  $y_0 = 0$ . The choice of 850 mb was chosen arbitrarily to represent the low level. According to the profile of  $Z(z)$  shown in Fig. 1, upper tropospheric fields have the opposite sign and approximately twice the magnitude of the lower tropospheric fields. Some prominent features are apparent in the decomposition of wave components. The total  $u, v, \phi$  fields are composed of Rossby waves on the west side of the source, Kelvin waves on the east side, with “slaved” inertia-gravity waves providing low-level convergence near the source. An interesting property of these simple linear solutions is that the lower tropospheric maximum westerly winds in the wake of the convective envelope are stronger than the lower tropospheric maximum easterly winds ahead of the convection. Also notable is the larger zonal extent of the easterlies compared with the westerlies. These characteristics agree well with the observed MJO composite presented by Kiladis et al. (2005, their Fig. 3).

## 3. AN INVERTIBILITY PRINCIPLE

We now show that the wind and mass fields in the wake of a convective envelope can be approximately recovered from the PV through a simple invertibility principle. The argument begins by returning to (3), written in the form

$$\nabla^2\psi + \frac{\beta y}{RT} \left( \frac{\partial}{\partial z} - 1 \right) \frac{\partial\phi}{\partial z} = q, \quad (5)$$

where  $\psi$  is the streamfunction for the rotational part of the flow and  $\nabla^2 = \partial^2/\partial x^2 + \partial^2/\partial y^2$  is the horizontal Laplacian operator. Equation (5) can be

converted into an invertibility principle by introducing an approximate balance relation between the wind and mass fields, i.e., a relation between  $\psi$  and  $\phi$ . The balance approximation used here is derived from the linear balance relation  $\nabla \cdot (\beta y \nabla \psi) = \nabla^2 \phi$ , with the additional assumption that  $\beta y$  can be treated as slowly varying. With this additional assumption, the linear balance approximation can be written as  $\nabla^2(\phi - \beta y \psi) = 0$ , from which, with the condition  $\phi - \beta y \psi \rightarrow 0$  as  $y \rightarrow \pm\infty$ , it immediately follows that  $\phi = \beta y \psi$ . Using this in (5) we obtain

$$\nabla^2 \psi + \frac{\beta^2 y^2}{R\Gamma} \left( \frac{\partial}{\partial z} - 1 \right) \frac{\partial \psi}{\partial z} = q. \quad (6)$$

Concerning the boundary conditions for (6), we here use the simple conditions  $\psi \rightarrow 0$  as  $y \rightarrow \pm\infty$  and  $\partial\psi/\partial z = 0$  at  $z = 0, z_T$ . Equation (6), together with its boundary conditions, constitute an invertibility principle. From this principle we can recover  $\psi$ , and then compute the rotational wind field from  $(u_\psi, v_\psi) = (-\partial\psi/\partial y, \partial\psi/\partial x)$  and the mass field from  $\phi = \beta y \psi$ . Although the invertibility principle (6) can be used in conjunction with an approximate PV equation to form a closed balanced theory, our discussion in this section is limited to the use of (6) as a diagnostic aid for interpretation of the primitive equation model results. The mathematical procedure for solving (6) is similar to that for solving the primitive equations, for details see Schubert and Masarik 2006. For the PV field we use the Rossby wave contribution to the total PV computed from the primitive equation solutions. This is a reasonable approximation since the total PV is dominated by the Rossby wave contribution.

A plot of the Rossby wave contribution to  $q(\xi, y, z)$  due to a heat source centered on the equator is shown in the first panel of Fig. 3. This solution illustrates how a propagating convective region leaves in its wake two trailing PV strips on opposite sides of the equator. In the second panel of Fig. 3,  $u_\psi(\xi, y, z)$ ,  $v_\psi(\xi, y, z)$ , and  $\phi(\xi, y, z)$  are shown, again for  $y_0 = 0$ . A comparison of the second panel in Fig. 2 with the second panel of Fig. 3 shows that the balanced model mass field and rotational wind field are fairly good approximations of the Rossby wave contributions to the primitive equation results. The most apparent difference being that the zonal pressure gradient force at the equator in the primitive equation model is not reproduced in the solutions of the invertibility principle.

#### 4. PARAMETERS CONTROLLING THE PV WAKE

Equation (2) states that  $q$  changes locally in time due to the Rossby term  $\beta v$ , the damping term  $-\alpha q$ , and the generation term  $(c_p \Gamma)^{-1} \beta y (\partial/\partial z - 1) Q$ . Insight into the importance of the  $\beta v$  term and into the critical parameters governing the PV wake can be obtained by calculating the hypothetical PV distribution that would result from forcing and dissipation only, i.e., the PV distribution resulting from the neglect of the Rossby term in (2). With the  $\beta v$  term neglected, and with the replacement  $\partial/\partial t \rightarrow -c(\partial/\partial \xi)$ , (2) reduces to

$$c \frac{\partial q}{\partial \xi} = \alpha q - \frac{\beta y}{c_p \Gamma} \left( \frac{\partial}{\partial z} - 1 \right) Q, \quad (7)$$

The solution of (7) is easily obtained and can be written in the form

$$q(\xi, y, z) = -\frac{\tau_p}{\tau_c} \left( \frac{\pi^2}{\pi^2 + \alpha^2 \tau_p^2} \right) F(\xi) \beta y \exp \left[ - \left( \frac{y - y_0}{b_0} \right)^2 \right] Z(z). \quad (8)$$

For the present discussion, details of  $F(\xi)$  are not necessary and will be omitted here. The PV field constructed from (8) at 850 mb and  $y_0 = 0$  is shown in Fig. 4. A comparison of Fig. 4 with the top panel of Fig. 3 shows that the neglect of  $\beta v$  results in a  $q$  field that has only 68% of the correct strength and does not extend far enough in the poleward direction. The lower tropospheric meridional flow shown in Fig. 2 extends poleward a considerable distance and results in an advection of basic state PV towards the equator. This effect, included in the PV field of Fig. 3, but excluded from Fig. 4, tends to make the PV anomaly stronger and broader in north-south extent.

In spite of this weakness, the solution (8) reveals an important parameter controlling the strength of the PV wake, namely the ratio of time scales  $\tau_p/\tau_c$ . The parameter  $\tau_p = a_0/c$  is a measure of the passage time of the convective region and the parameter  $\tau_c = \bar{c}^2/(\kappa Q_0)$  is a measure of the convective overturning time, where  $\bar{c}$  is the gravity wave phase speed corresponding to the first internal vertical mode. Thus, the ratio is a measure of the number of convective overturnings during the passage of the convection. The factor  $\tau_p/\tau_c$  is large, and the corresponding PV anomaly is large, for intensely

raining, zonally wide, slowly moving convective regions, while it is small, and the corresponding PV anomaly is small, for weakly raining, zonally narrow, fast moving convective regions. For the case shown in Fig. 4,  $a_0 = 1250$  km and  $c = 5$  ms<sup>-1</sup> so that  $\tau_p = 69.4$  hr, while  $\bar{c} = 41.25$  ms<sup>-1</sup> and  $Q_0/c_p = 12$  K day<sup>-1</sup> so that  $\tau_c = 11.9$  hr, resulting in  $\tau_p/\tau_c = 5.8$ .

## 5. CONCLUDING REMARKS

We have used a linear, equatorial  $\beta$ -plane, primitive equation model as a tool to investigate the large-scale wind and mass fields around a moving heat source near the equator. Within the context of the assumed linear dynamics, these fields have been decomposed into Rossby, mixed Rossby-gravity, inertia-gravity, and Kelvin modes. The Rossby modes are responsible for the flow pattern west of the moving convective envelope, Kelvin modes for the flow pattern east of the convection, and inertia-gravity modes for the divergent flow near the convection, with mixed Rossby-gravity modes playing a minor role when the convection is centered near the equator. The potential vorticity field is almost entirely associated with the Rossby modes and has a form crudely analogous to the pair of wing-tip vortices behind a large airplane. Although the patterns produced here by the primitive equation model are qualitatively similar to those found using the long wave approximation (e.g., Gill 1980, Heckley and Gill 1984, Gill and Philips 1986, Philips and Gill 1987, Chao 1987), they are more accurate because the long wave approximation distorts the dispersion relation for Rossby waves (e.g., Fig. 1 of Stevens et al. 1990).

We have proposed an equatorial invertibility principle as a method to approximately recover the balanced wind and mass fields from the PV field. Solution of this invertibility principle confirms that the flow in the wake of an eastward-moving equatorial convective envelope is essentially described by balanced dynamics.

Lastly, the magnitudes of the PV anomalies trailing behind the convective region depend on  $\tau_p/\tau_c$ , the ratio of the passage time to the convective overturning time. The passage time  $\tau_p$  is large if the convection moves slowly and has large zonal extent, while the overturning time is small if the apparent heat source and surface rainfall are large. Such convection produces large PV anomalies and a large equatorial westerly wind burst in its wake.

## ACKNOWLEDGMENTS

The author is grateful for the guidance of Wayne Schubert, and the help and advice from Brian McNoldy, Paul Ciesielski, and Tom Vonder Haar. This research was supported by the National Science Foundation under Grant ATM-0332197 and by the DoD Center for Geosciences/Atmospheric Research under Cooperative Agreement DAAD19-02-2-0005.

## 6. REFERENCES

- Chao, W. C., 1987: On the origin of the tropical intraseasonal oscillation. *J. Atmos. Sci.*, **44**, 1940–1949.
- Gill, A. E., 1980: Some simple solutions for heat induced tropical circulation. *Quart. J. Roy. Meteor. Soc.*, **106**, 447–462.
- Gill, A. E., and Philips, P. J., 1986: Nonlinear effects on heat induced circulation of the tropical atmosphere. *Quart. J. Roy. Meteor. Soc.*, **112**, 69–91.
- Hausman, S. A., Ooyama, K. V., and Schubert, W. H., 2005: Potential vorticity structure of simulated hurricanes. *J. Atmos. Sci.*, **62**, in press.
- Heckley, W. A., and Gill, A. E., 1984: Some simple analytic solutions to the problem of forced equatorial long waves. *Quart. J. Roy. Meteor. Soc.*, **110**, 203–217.
- Hendon, H. H., and Salby, M. L., 1994: The life cycle of the Madden-Julian oscillation. *J. Atmos. Sci.*, **51**, 2225–2237.
- Johnson, R. H., and Ciesielski, P. E., 2000: Rainfall and radiative heating rates from the TOGA COARE atmospheric budgets. *J. Atmos. Sci.*, **57**, 1497–1514.
- Kiladis, G., Straub, K. H., and Haertel, P. T., 2005: Zonal and vertical structure of the Madden-Julian oscillation. *J. Atmos. Sci.*, **62**, 2790–2809.
- Lin, X., and Johnson, R. H., 1996b: Heating, moistening, and rainfall over the western Pacific warm pool during TOGA COARE. *J. Atmos. Sci.*, **53**, 3367–3383.
- Philips, P. J., and Gill, A. E., 1987: An analytic model of the heat-induced tropical circulation in the presence of a mean wind. *Quart. J. Roy. Meteor. Soc.*, **113**, 213–236.
- Schubert, W. H., Ciesielski, P. E., Stevens, D. E., and Kuo, H.-C., 1991: Potential vorticity modeling of the ITCZ and the Hadley circulation. *J. Atmos. Sci.*, **48**, 1493–1509.
- Schubert, W. H., Masarik, M. T., 2006: Potential Vorticity Aspects of the MJO. *Dynamics of Atmospheres and Oceans*, in press.
- Stevens, D. E., Kuo, H.-C., Schubert, W. H., and Ciesielski, P. E., 1990: Quasi-balanced dynamics in the tropics. *J. Atmos. Sci.*, **47**, 2262–2273.

Yanai, M., Chen, B., and Tung, W.-W., 2000:  
The Madden-Julian oscillation observed during the  
TOGA COARE IOP: Global view. *J. Atmos. Sci.*,  
**57**, 2374–2396.

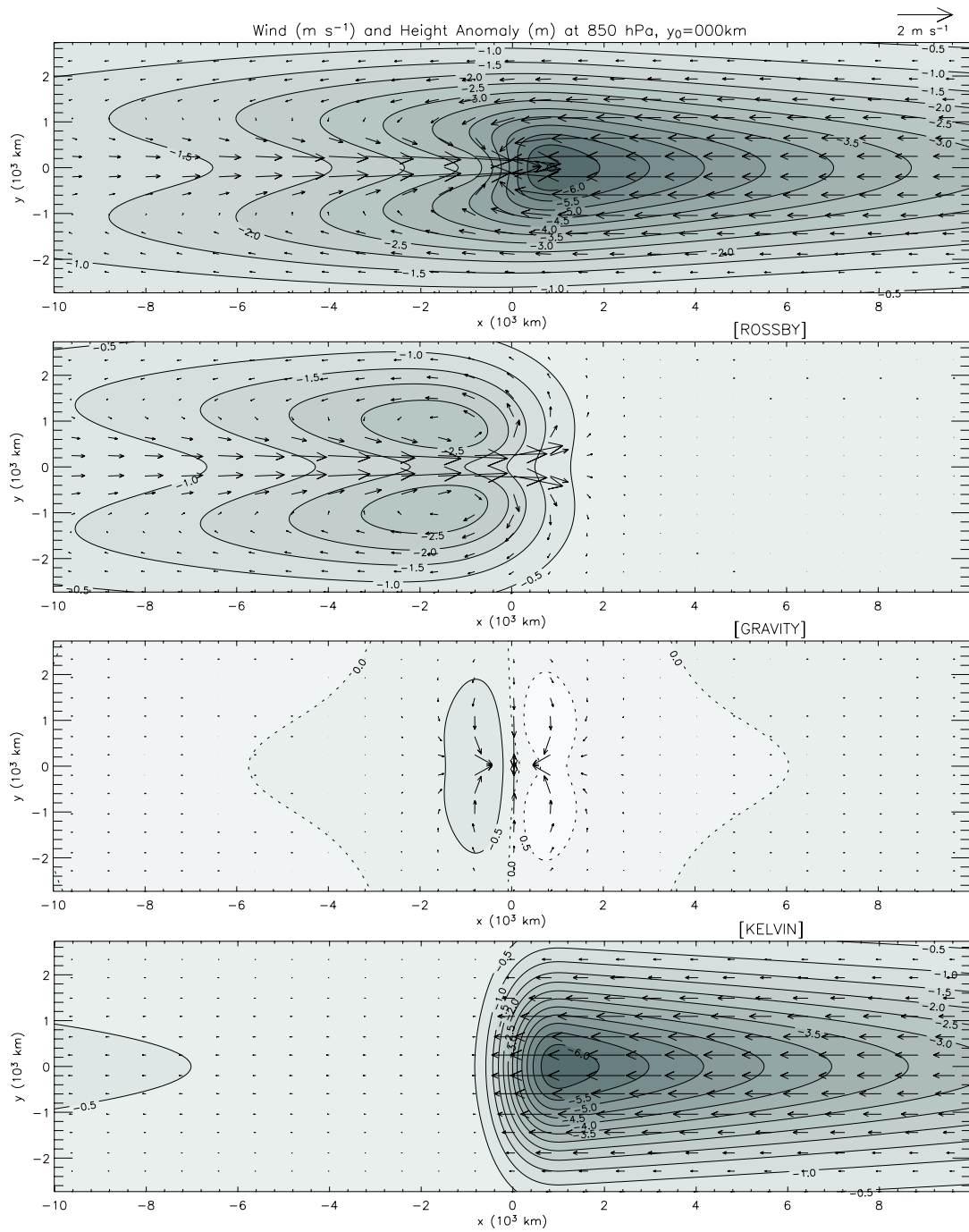


Figure 2: The upper panel shows the geopotential height anomaly and winds at 850 mb for  $y_0 = 0$ . The remaining three panels show respectively the contributions made by Rossby waves, inertia-gravity waves, and Kelvin waves.

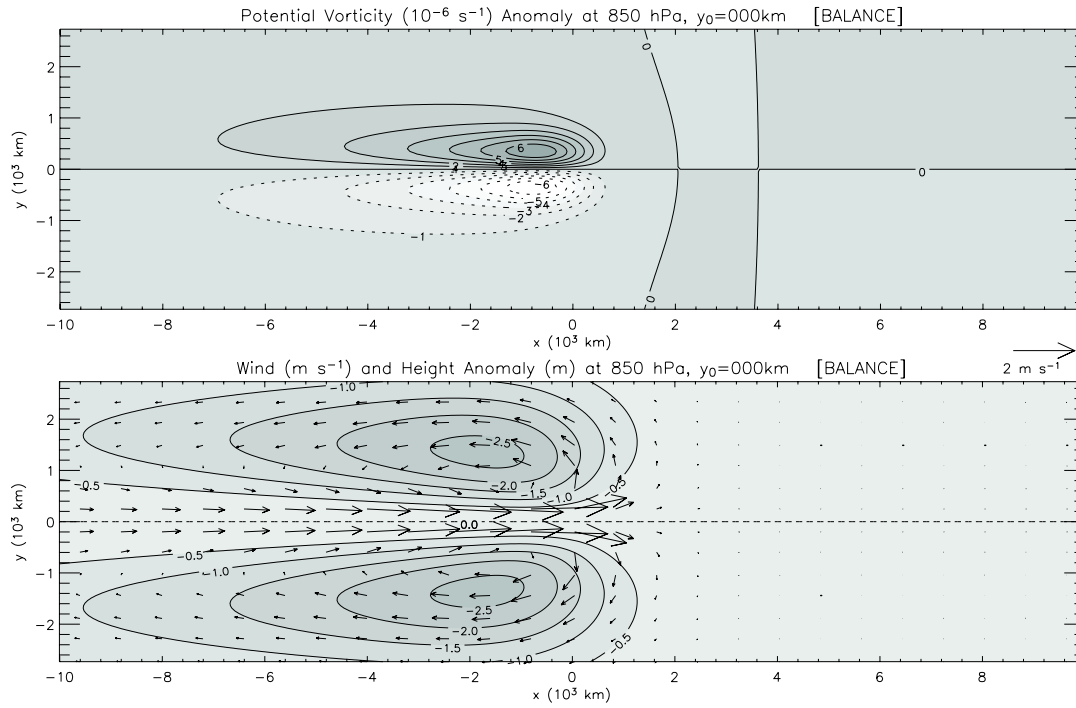


Figure 3: The top panel shows the Rossby wave contribution to the  $q(\xi, y, z)$  field, while the second panel shows the  $u_\psi(\xi, y, z)$ ,  $v_\psi(\xi, y, z)$ ,  $\phi(\xi, y, z)$  fields resulting from the solution of the invertibility principle (6) when its right hand side is given by the PV field shown in the top panel. This figure is for  $y_0 = 0$ .

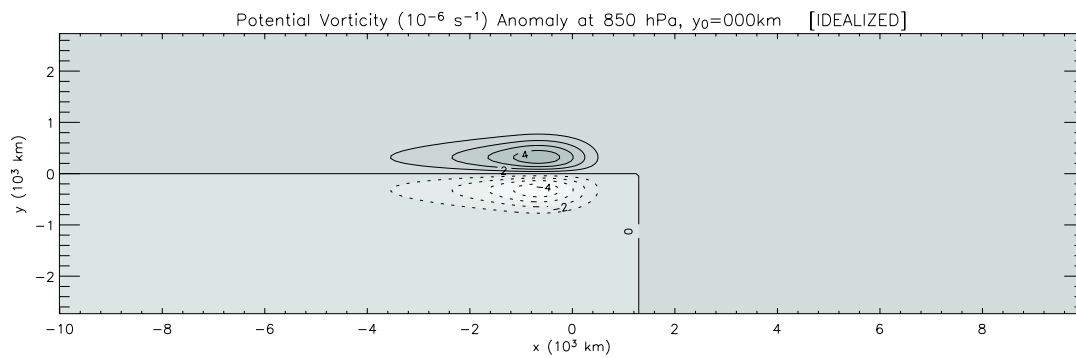


Figure 4: Hypothetical potential vorticity resulting from forcing and dissipation only, as computed from (8) with  $y_0 = 0$ .